The partitioning of gross primary production for *Eucalyptus tereticornis* trees exposed to experimental warming and drought

John E. Drake[1,2*], Mark G. Tjoelker[1], Michael J. Aspinwall[1,3], Peter B. Reich[1,4], Sebastian Pfautsch[1,5], Craig V. M. Barton[1]

[1]Hawkesbury Institute for the Environment, Western Sydney University, Locked Bag 1797, Penrith NSW 2751, Australia
[2]Forest and Natural Resources Management, SUNY-ESF, 1 Forestry Drive, Syracuse, NY, 13210 USA.
[3]Department of Biology, University of North Florida, 1 UNF Drive, Jacksonville, FL, 32224 USA.
[4]Department of Forest Resources, University of Minnesota, 1530 Cleveland Ave N., St Paul, MN, 55108 USA.
[5]School of Social Science and Psychology (Urban Studies), Western Sydney University, Locked Bag 1797, Penrith, NSW 2751, Australia.

[*]Corresponding author. Email: jedrake@esf.edu, telephone: 415-470-6574

Word counts:

Main text (Intr-Ack):	6528
Summary:	199
Introduction:	1278
Materials and Methods:	2261
Results:	1326
Discussion:	1540
Acknowledgements:	123

8 figures, 1 tables, and supporting information.

Summary

- The allocation of C is an important component of tree physiology that influences growth and ecosystem C storage. Allocation is challenging to measure and the influences of environmental changes such as warming and drought are uncertain.
- We exposed *Eucalyptus tereticornis* trees to a factorial combination of +3°C warming and an extreme summer drought in the field using whole-tree chambers. We calculated C allocation terms using detailed measurements of growth and continuous whole-crown CO_2 and H_2O exchange measurements.
- Warming accelerated growth and leaf area development, and increased the partitioning of Gross Primary Production (GPP) to aboveground respiration and growth, while decreasing partitioning belowground. The summer drought reduced C gain and growth, but did not impact GPP partitioning. Trees utilized deep soil water and avoided strongly negative water potentials during the drought.
- Warming increased growth respiration, but maintenance respiration acclimated homeostatically. The increasing growth rates of trees in the warmed treatment resulted in higher rates of respiration, even with complete acclimation of maintenance respiration.
- Warming-induced stimulations of tree growth likely involve increased C allocation aboveground, particularly to leaf area development, while reduced water availability may not stimulate allocation to roots.

Introduction

The C economy of trees and forests depends not only on the amount of C fixed via photosynthesis, but how that fixed C is used. Ecosystem C storage is affected by the allocation of C to long-lived C pools such as wood relative to C allocation to pools with higher turnover rates such as fine roots (DeLucia *et al.*, 2005). C allocation also affects the acquisition of light, nutrients, and water, which influences ecosystem C cycling (Litton *et al.*, 2007; Epron *et al.*, 2012; Franklin *et al.*, 2012; De Kauwe *et al.*, 2014). The allocation of C belowground affects soil C and nutrient cycling (Högberg *et al.*, 2001; Epron *et al.*, 2012) in part because belowground C allocation can affect soil organic matter decomposition and the acquisition of limiting nutrients by trees (Drake *et al.*, 2011; Finzi *et al.*, 2015). The importance of C allocation and the relative difficulty of its study contribute to its role as an important unknown for modeling the biogeochemistry of ecosystems (Roux *et al.*, 2001; Franklin *et al.*, 2012; Dietze *et al.*, 2014; De Kauwe *et al.*, 2014).

Terminology regarding allocation has been a source of some confusion. Here, we follow Litton *et al.* (2007) and use 'allocation' as a term of broad definition encompassing three specific aspects of study: (1) *ratios* of biomass pool sizes, (2) *fluxes* of C to a given component, and (3) *partitioning*, the C flux to a given component as a fraction of GPP. These areas of study are similar, but not equivalent. For example, old and large trees have a large wood mass fraction relative to small young trees (Poorter *et al.*, 2015), but this reflects the low turnover of woody tissues relative to leaves, not a higher partitioning of GPP to wood in old trees (Duursma & Falster, 2016). Thus it is often inappropriate to infer C partitioning from biomass ratios (Reich, 2002; Litton *et al.*, 2007). Surprisingly, partitioning of photosynthate is relatively poorly understood despite its direct relevance to ecosystem models (Epron *et al.*, 2012; Franklin *et al.*, 2012; De Kauwe *et al.*, 2014).

Several schemes have been used to conceptualize and model C allocation. The simplest approach is to assume that trees partition a constant fraction of fixed C to each use (e.g., growth, respiration). This is supported by linear relationships between production terms in some systems (Gower *et al.*, 2001). However, fixed allocation schemes cannot capture ontogenetic effects (Poorter *et al.*, 2015; Duursma & Falster, 2016) or dynamic temporal responses (De Kauwe *et al.*, 2014; Doughty *et al.*, 2014). Another approach is to assume a functional balance between tree organs via allometric relationships, Huber values, or root to leaf mass fractions (Landsberg & Waring, 1997; Mäkelä *et al.*, 2008; Feng *et al.*, 2012). Finally, there is the concept that trees increase C partitioning towards the acquisition of the primary limiting resource (McMurtrie & Dewar, 2013). This approach appears sensible and has been implemented in several models (e.g., Running & Gower, 1991; Friedlingstein *et al.*, 1999), but direct evidence supporting

this concept is scarce, given the challenges involved in measuring allocation (Poorter & Sack, 2012; Poorter *et al.*, 2015). However, optimization approaches have been used to constrain dynamic allocation schemes with some success (Franklin *et al.*, 2012; McMurtrie & Dewar, 2013).

Temperature is a fundamental aspect of climate that affects many aspects of tree physiology (Way & Oren, 2010; Lu *et al.*, 2013). Several lines of evidence suggest that warming may increase tree C allocation aboveground at the expense of C allocation belowground. Experimental warming of forest soil increased aboveground biomass while reducing or not affecting belowground biomass (Strömgren & Linder, 2002; Melillo *et al.*, 2011), which has been attributed to a warming-induced increase in soil N availability (Melillo *et al.*, 2002). A recent ^{13}C-CO_2 labeling study indicated that warming increased allocation aboveground and reduced C allocation belowground in beech saplings via a direct effect on tree physiology, without an altered soil N cycle (Blessing *et al.*, 2015). Also, environmental gradients in mean annual temperature are strongly correlated with the distribution of biomass; forests have a lower root mass fraction (i.e., the proportion of live forest biomass contained in roots) in warm climates than in cold climates (Reich *et al.*, 2014). Meta-analyses of warming experiments generally found an increase in aboveground plant growth (Rustad *et al.*, 2001) that is slightly larger than the increase in belowground plant growth (Lu *et al.*, 2013), although such experiments have exclusively involved small stature vegetation given the logistical challenges of warming tall forests. Thus, prior research suggests a shift in C allocation aboveground with experimental warming, although direct tests in the field with large trees have not yet been performed.

Water availability also impacts tree growth and physiology (e.g., Mencuccini, 2003; Nemani *et al.*, 2003; Farooq *et al.*, 2009) and the effects of drought are of particular concern (Burke *et al.*, 2006; Sillmann *et al.*, 2013). While it appears sensible that trees would increase C allocation to roots in dry regions or during drought periods (Poorter *et al.*, 2012), there is limited support for this idea. Reich *et al.* (2014) found no correlation between root mass fraction and aridity across a global dataset of >6,200 forests. Additionally, Amazonian forests responded to droughts in 2005 and 2010 with a shift away from fine-root growth and increased C partitioning to aboveground growth and respiration, particularly in the year following the drought (Doughty *et al.*, 2014, 2015). However, drought has been observed to increase root mass fractions for small plants grown in artificial conditions (Reich, 2002; Poorter *et al.*, 2012), and increased C allocation belowground under drought is consistent with some ^{13}C-CO_2 labeling studies (Hommel *et al.*, 2016), but not others (Hartmann *et al.*, 2015). While the simple expectation of increased allocation to roots during drought is appealing, C allocation responses to drought are likely more complex and merit further study.

Interactions between temperature and drought effects may also be important for tree C allocation. Warmer temperatures may exacerbate tree H_2O loss during drought and increase mortality risk (Allen *et al.*, 2015). If warmer temperatures reduce C allocation belowground, then the ability of trees to acquire soil water may also be impaired. However, an open top chamber experiment with young oak saplings found no interaction between experimental warming and drought on tree transpiration or biomass (Kuster *et al.*, 2013). Other studies have found limited evidence for interactive effects on plant growth rates (e.g., Edler *et al.*, 2015; Taeger *et al.*, 2015), although there are also exceptions (Munir *et al.*, 2015; Leon-Sanchez *et al.*, 2016). A six-year warming and precipitation redistribution experiment with two tree species found complex growth responses (Volder *et al.*, 2013) with a strongly interactive effect on the relative growth rate of *Quercus stellata* monocultures. Thus, it is challenging to generalize how the interactive effects of drought and warming affect tree physiology and growth.

To address these knowledge gaps concerning, temperature, water availability, and C allocation, we studied C allocation in 8 to 9-meter tall eucalypt trees growing in an experiment that manipulated both temperature and moisture supply. We used whole-tree chambers in the field in southeastern Australia to grow *Eucalyptus tereticornis* trees under experimental warming of +3 ^{o}C for more than one year, crossed with a summer drought for three months. We continuously measured whole-crown CO_2 and H_2O exchange and measured aboveground biomass production every 2 weeks. From these intensive measurements, we derived GPP, aboveground net primary production (NPP_a), aboveground autotrophic respiration (R_a) and the residual C that must have been partitioned belowground for each fortnightly interval. We use these data to test the predictions that warming decreases C partitioning belowground, while drought increases C partitioning belowground.

Materials and Methods

Site and experiment

We implemented a warming and drought experiment using 12 whole-tree chambers (WTCs) in Richmond, New South Wales (Australia; 33°36′40″S, 150°44′26.5″E). The WTCs were large cylindrical structures topped with a cone (3.25 m in diameter, 9 m in height, volume of ~53 m^3) that enclosed a single tree rooted in soil. The WTCs controlled atmospheric CO_2 concentration, air temperature (T_{air}), relative humidity (RH), and irrigation while continuously measuring the net exchange of CO_2 and H_2O between entire tree crowns and the atmosphere (Barton *et al.*, 2010; Duursma *et al.*, 2011; Barton *et al.*, 2012; Duursma *et al.*, 2014; Drake *et al.*, 2016b; Aspinwall *et al.*, 2016).

The roots of each tree were compartmentalized with a barrier extending vertically belowground to 100-cm-depth. A cemented layer of manganese nodules and clay was present at 90–100 cm depth, providing a natural horizontal barrier at the bottom of the rooting volume. Thus, the rooting volume of each tree was isolated from surrounding trees. However, some trees extended roots through this layer and acquired deep soil water in a previous experiment (Duursma *et al.*, 2011). Soil was collected from an adjacent paddock and placed in the chambers in two layers (0–25 cm and from 25 cm to the hard layer) on 10 July 2012. Soils at the site were an alluvial formation of low-fertility sandy loam (Clarendon sand).

Nursery seedlings of a local provenance of *Eucalyptus tereticornis* Sm. were established in 25 L pots inside the WTCs using the same soil. *Eucalyptus tereticornis* was chosen because it is a widespread and abundant tree across eastern Australia (Drake *et al.*, 2015). Six potted trees were placed in each chamber on 5 December 2012; a single tree was selected based on size similarity within each treatment and planted in the chamber center on 12 March 2013. Trees assigned to the ambient and warmed temperature treatments had equivalent height and basal diameter when potted seedlings were placed into the WTCs in December 2012 (heights of 41.5 ± SE of 0.8 and 40.2 ± 1.8 cm; diameters of 2.4 ± 0.1 and 2.5 ± 0.1 mm in ambient and warmed treatment, respectively).

Six chambers tracked ambient T_{air} and six chambers tracked ambient T_{air} + 3°C warming (n = 6; 'ambient' and 'warmed'); treatments started on 12 December 2012 (Drake *et al.* 2016b; Aspinwall *et al.* 2016). The average warming achieved was +2.9 °C (± sd of 0.3 across 466 days) for T_{air}, +2.2 °C (± sd of 0.4) for soil temperature at 5-cm-depth, +2.0 °C (± sd of 0.4) for soil temperature at 20-cm-depth, and +1.4 °C (± sd of 0.2) for soil temperature at 50-cm-depth. Trees were irrigated equally every 15 d with half the mean monthly rainfall. A water exclusion treatment was applied to half of the trees on 12 February 2014, resulting in a 2x2 factorial design between the experimental treatments of warming and drought (n = 3; abbreviated A-Wet, A-Dry, W-Wet, and W-Dry hereafter). Trees assigned to the drought

treatment received no irrigation from 12 February 2014 through 5 May 2014, representing an extreme summer drought of nearly three months.

Plant water status and soil water content

Predawn leaf water potentials ($\Psi_{L\text{-}PD}$) were measured monthly prior to the drought and every one to two weeks during the drought treatment. Three leaves were measured per tree on each date using a Scholander-type pressure chamber (1505D-EXP; PMS Instrument Company, OR, USA). Leaves were placed in sealed and humidified plastic bags, placed in a dark cool box, and measured within one hour of collection in a nearby laboratory.

Soil volumetric water content was measured by three sensors in each chamber (CS650 time-domain reflectometers; Campbell Scientific, Logan, UT, USA). Sensors were installed horizontally at three depths: in the surface soil (10-cm-depth), at 30-cm-depth, and just above the hard layer of cemented manganese (~100-cm-depth). Soil temperature was measured with thermocouples at 5, 20, and 50-cm within the center of each chamber.

A single neutron probe per chamber (503DR, Hydroprobe, Instrotek, NC, USA) was used to measure soil water content to a depth of 425 cm (at 25 or 50 cm steps) approximately every two weeks (Duursma *et al.*, 2011). Note that high neutron probe counts in deep soil (150-400 cm depth) partially reflect a change in soil texture towards a higher clay content.

Whole tree crown flux measurements

An automated system measured the net exchange of CO_2 and H_2O between each crown and its chamber airspace (Barton *et al.*, 2010). Measurements began on 13 September 2013 when suspended plastic floors were sealed around the stem of each tree at ~45 cm height, when the trees were ~3 m tall. Flux measurements finished on 26 May 2014, when the trees were nearly 9 m tall. We report >70,000 hourly flux observations aggregated into >3000 daily sums across 12 trees.

We partitioned the net CO_2 fluxes into the components of GPP and R_a using an analytical technique common to eddy-covariance research (Reichstein *et al.*, 2005); see Drake *et al.* (2016b) for a complete description. We used direct measurements of whole-crown R_a and its temperature dependence at night to predict R_a for each hourly measurement as a function of T_{air}. For daylight hours, we then calculated GPP as the sum of the measured net CO_2 flux and the predicted R_a given the measured T_{air}. We assumed GPP was zero when PPFD = 0; in such conditions, the measured net C flux was used as the measure of R_a. Note that the chamber airspaces were continuously well-mixed and R_a fluxes were directly measured at night, avoiding some of the issues inherent in eddy covariance partitioning. The underlying flux data and the partitioning approach were published previously (Drake *et al.*, 2016ab).

Final harvest

The dry mass of all trees was measured destructively at the end of the experiment (26 May 2014). Total tree dry mass was measured as the sum of five components: leaves, branches, stem, coarse roots, and fine roots.

The crown of each tree was divided into three equal heights. All branches were cut flush to the stem and all leaves were separated from branches. A random subsample of 100 leaves per layer was measured for total leaf area (LI-3100C leaf area meter, LiCor, Lincoln, NE, USA), dry mass, and specific leaf area (SLA). The stem was cut into three segments and 1-cm-thick cross-sections (cookies) were sampled for bark depth, wood density, and bark density at the stem base, between the first and second layers, and between the second and third crown layers. Bark and wood density was measured on cookie subsamples (Thomas *et al.*, 2007). Wood and bark densities were similar (0.44 and 0.37 g cm^3 for wood and bark, respectively). Bark depth increased with stem diameter ($\log_{10}$(bark depth, mm) = -1.48 + 1.23 × $\log_{10}$(diameter, cm), P <0.001, r^2 = 0.92) while wood and bark density decreased with stem diameter (wood density = 0.50 – 0.001 × diameter, P = 0.007, r^2 = 0.17; bark density = 0.45 – 0.001 × diameter, P < 0.001, r^2 = 0.48; densities in g cm^3, diameter in cm). Warming and drought treatments did not alter these relationships (ANCOVA, P > 0.05). Total stem, branch, and leaf mass were measured directly after drying at 70 °C; some samples required >2 weeks of drying to reach a stable dry mass.

Fine roots were measured using soil cores. The soil surface area was divided into four equal quadrants and two 50-mm-diameter cores were taken within each quadrat on 29 May 2014, just after the crown harvest. Cores were separated into two depths: (1) 0-25 cm and (2) from 25 cm to the hard layer, which varied from 70 to 100 cm depth. Samples within each quadrat and depth category were composited (eight samples per chamber). Fine roots were isolated by washing samples through 2-mm and then 1-mm brass sieves; fine roots were defined as all roots < 2-mm-diameter. Fine root dry mass was measured after drying at 70 °C. Total fine root dry mass was calculated as the product of fine root density (g m^{-3}) and soil volume (m^3) in each layer.

Coarse roots were destructively harvested by fully excavating the soil volume of each chamber. Soil was shoveled out of the chamber onto a conveyor belt that transported the soil to a series of 5-mm steel sieves. Roots were collected by hand, washed, sorted into two size categories (2-10 mm, > 10 mm diameter), and weighed after drying at 70 °C.

Growth measurements

Aboveground biomass was estimated every two weeks for each tree as the sum of leaf, branch, wood, and bark mass; aboveground net primary production (NPP_a) was estimated as the fortnightly difference in aboveground biomass plus fortnightly litterfall, assuming a constant biomass C fraction of 0.5 of dry mass.

Tree height and stem volume were measured fortnightly; diameter was measured at 30-cm-intervals along each tree stem from a basal height of 15-cm (prior to floor installation) or 65-cm (after floor installation) to the tree apex. The volume of stem wood and bark was estimated for each stem segment as the frustum of a cone, corrected for bark depth (*see above*). Wood and bark mass were calculated as the product of volume and density.

An allometric relationship was developed to predict branch wood mass from branch diameter based on destructively sampled branches on 13 May 2014 and 22 May 2014 ($\log_{10}$(branch mass) = -1.299 + 2.722 × $\log_{10}$(branch diameter), $P < 0.001$, $r^2 = 0.91$, branch mass in g, branch diameter in mm, n = 48 branches). This allometry did not differ between treatments (ANCOVA, $P > 0.1$) and was used to predict total branch mass on three dates when the diameter of all branches was measured (24 Oct 2013, 15 Jan 2014, and 22 May 2014). Total branch mass and stem volume were strongly correlated in a chamber specific manner (log-log ANCOVA, $P < 0.001$, $r^2 = 0.95$), which was used to estimate branch mass as a function of stem volume.

Standing leaf area and leaf mass production were estimated as previously at this site (Barton *et al.*, 2012; Drake *et al.*, 2016b). Standing leaf area was measured for each tree by counting all the leaves and multiplying by a tree-specific mean leaf size measured across the crown of each tree with a handheld leaf area meter (LI-3000; n = 86 to 102 leaves per tree). These measurements were performed prior to chamber floor installation (9 Sept 2013) and at the beginning of the drought treatment (10 Feb 2014). A third direct measurement of standing leaf area was calculated from the final harvest data (26 May 2014) by multiplying total crown leaf dry mass by SLA weighted by the leaf dry mass in each layer. Litterfall was collected, dried, and weighed fortnightly for each tree, although relatively few leaves fell as litter (~5% of the total leaf mass). Total tree leaf mass was estimated for each set of fortnightly size measurements by dividing leaf area by the crown-weighted SLA measured at harvest.

Calculating C partitioning

A major goal of this study was to calculate the partitioning of photosynthetically fixed C into components for each fortnightly interval. We quantified GPP, NPP_a, and R_a separately, as described above. We calculated the residual between GPP and the sum of NPP_a and R_a:

$$GPP = NPP_a + R_a + residual \quad \text{(eq. 1)}$$

The residual term is a mass-balance calculation of all C put belowground to root production, respiration, and exudation, but this term is also affected by measurement error in GPP, NPP_a, and R_a. We calculated the partitioning of GPP directly for each fortnightly interval as NPP_a/GPP, R_a/GPP, and residual/GPP.

Growth and maintenance R_a

Given the evidence for thermal acclimation of tissue-specific respiration rates to experimental warming in this experiment (Drake *et al.*, 2016b; Aspinwall *et al.*, 2016), we investigated growth and maintenance respiration as drivers of R_a (McCree, 1970; Tjoelker *et al.*, 1999; Amthor, 2000; Adu-Bredu & Hagihara, 2003). We evaluated the relationship between R_a per unit tree C and relative growth rate (RGR); the slope reflects the growth component of R_a, while the y-intercept reflects the maintenance component of R_a. If R_a does not acclimate to warming, we expect the warmed treatment to have a higher y-intercept than the ambient treatment. If R_a acclimates homeostatically, we expect the ambient and warmed treatments to have equivalent intercepts. We also directly estimated coefficients associated with growth and maintenance components of R_a (Amthor, 2000);

$$R_a = R_g + R_m = g_r G + m_r W \qquad \text{(eq. 2)}$$

where R_g is the growth respiration rate (gC d^{-1}), R_m is the maintenance respiration rate (gC d^{-1}), G is biomass growth (gC d^{-1}), W is the standing biomass weight (gC), g_r is the growth respiration coefficient (gC respired per gC growth), and m_r is the maintenance respiration coefficient (gC respired per gC standing biomass d^{-1}).

Data analysis

Data were analyzed following a completely randomized design with the single treatment of warming (n = 6 for 6 months, then n = 3 for the drought period). Longitudinal analyses were performed using the 'lme' function within the 'NLME' R package with a random tree effect and fixed effects of date, temperature treatment, and water treatment. Treatment means were estimated after adjustment for other terms in the model (i.e. least square means, or LS means) with the 'LSMEANS' package in R v.3.2.2 (R Development Core Team, 2012; Pinheiro et al., 2013). Analyses were evaluated to test assumptions of residual normality and homoscedasticity; transformations were often necessary. Datasets that were not longitudinal were analyzed as a 2x2 ANOVA using the 'lm' function in R. Equation 2 was fit using the 'NLME' R package with a random tree effect.

Results

Growth

Experimental warming increased the rates of diameter and height growth (Fig. 1a,b), particularly during the Austral winter and spring. Trees in the warmed treatment were larger than trees in the ambient treatment when the CO_2 and H_2O flux measurements began (13 Sept 2013; vertical dashed line in Fig. 1). On that date, warming had increased diameter by 21% ($P < 0.01$; Fig. 1a), height by 19% ($P < 0.01$; Fig. 1b), total leaf area by 53% ($P < 0.01$; Fig 1c), and stem volume by 79% ($P < 0.01$; Fig 1d). During the warm summer, the diameter and height of the ambient and warmed treatment trees converged (Fig. 1a,b), but total stem volume continued to be larger in the warmed treatment (Fig. 1d). This effect was driven by a difference in stem taper- the warmed trees had wider stem diameters throughout the crown than the ambient trees (*not shown*). The drought treatment reduced tree diameter but not height growth (Fig. 1a,b), modestly reduced total leaf area (Fig. 1c), and reduced stem volume increment (Fig. 1d). Notably, there was no interactive effect of warming and drought on growth (e.g., $P > 0.4$ for volume increment).

CO_2 and H_2O fluxes

Experimental warming increased photosynthetic C uptake and H_2O loss via transpiration early in the experiment (Fig. 2a,c). This was expected, given the strong increase in tree growth and total leaf area with experimental warming during this period (Fig. 1). However, the rates of C uptake and H_2O loss converged between the ambient and warmed treatments during the summer (January; Fig. 2a,c), despite the fact that the warmed trees were larger and had more leaf area. This may have been influenced by warming-induced reductions in photosynthetic rates per unit leaf area (Drake *et al.*, 2016b).

We imposed an experimental drought in which all surface irrigation was withheld from trees in the dry treatments for nearly three months. Total C uptake during the drought period was reduced 25% while total H_2O loss was reduced 32% (Fig. 2b,c; main effects of drought, $P < 0.01$; no interaction with warming, $P > 0.5$). Thus, the drought strongly and significantly reduced whole-crown fluxes of C uptake and H_2O loss. On the other hand, these fluxes were maintained at moderate values during the drought, despite the complete lack of water addition.

Final harvest

The final biomass did not differ between the warming or drought treatments (Fig. 3a). The lack of difference in final mass between the ambient and warmed treatments may have arisen from the convergence of tree diameter and height across treatments (Fig. 1a,b). The difference in stem volume between ambient and warmed trees (Fig. 1d) was apparent in the harvest biomass (Fig. 3a), but was not statistically significant at this level of replication ($n = 3$; $P > 0.05$). The only biomass component that was affected by the experimental treatments at harvest was fine root biomass, for which there was a significant

interaction between warming and drought ($P < 0.05$). The A-Dry trees had higher fine root biomass than the A-Wet trees, while the W-Dry trees had slightly lower fine root biomass than the W-Wet trees (Fig. 3a). This interaction was also present in the tree root mass ratios; experimental drought increased the root mass ratio, but only in the ambient temperature treatment ($P < 0.05$; Fig. 3b).

Plant and soil water status

The drought reduced soil volumetric water content from 10-100 cm depth to values approaching 0.05 m^3 m^{-3} (Fig. 4a-c). Pre-dawn leaf water potentials ($\Psi_{L\text{-}PD}$) were reduced in the dry treatments relative to the wet treatments (Fig. 4d; $P < 0.01$). However, this effect was modest; $\Psi_{L\text{-}PD}$ was -0.29 ± 0.02 in the control and -0.48 ± 0.05 in the dry treatments. Thus, the drought trees had moderate $\Psi_{L\text{-}PD}$ (Fig. 4d) and moderate rates of transpiration (Fig. 2c) despite extremely dry surface soils.

Trees likely utilized deep soil water during the drought treatment. We observed a few roots of approximately 1-cm-diameter penetrating through the cemented manganese layer at ~100 cm depth during the complete soil excavation (JE Drake, *personal observation*). Neutron probe measurements down to 400-cm-depth indicated that soil water was removed from the profile in the dry treatment chambers during the drought, particularly from 50- to 200-cm-depth (Fig. S1). Thus, trees in the dry treatments likely transpired deep soil water during the summer drought, consistent with a previous drought study of *Eucalyptus saligna* at this site (Duursma *et al.* 2011).

Fluxes of GPP, NPP_a, R_a and allocation belowground

We derived gross primary production (GPP) and its partitioning to aboveground net primary production (NPP_a), aboveground autotrophic respiration (R_a), and the residual, which we attribute to C allocation belowground as well as measurement error.

GPP was increased by experimental warming early in the experiment (+22%, $P < 0.01$), but GPP between ambient and warmed treatments converged beginning in mid-summer (late January; Fig. 5a). The drought treatment reduced GPP in both temperature treatments (-15%, $P < 0.01$). These results follow the net C flux measurements (Fig. 2a,c). The response of NPP_a (Fig. 5b) closely followed the results for GPP, with a warming effect early in the experiment (+36%, $P < 0.01$) and a reduction with drought in both temperature treatments (-25%, $P < 0.01$). The response of R_a (Fig. 5c) also followed GPP, with a stimulation by warming early in the experiment (+39%, $P < 0.01$) and a modest reduction with drought that was equivalent across temperature treatments (-13%, $P < 0.05$). The allocation of C belowground, as measured by the residual, was decreased by experimental warming throughout the experiment (-11%, $P < 0.05$) and was unchanged by the drought treatment (+3%, $P > 0.1$; Fig. 5d).

GPP partitioning

Given these flux measurements, we derive the partitioning of GPP into three components; NPP_a/GPP, R_a/GPP, and Residual/GPP (Figs. 6-7). Warming increased NPP_a/GPP in a way that was stronger early in the experiment (+11%, $P = 0.01$) relative to the entire experiment (+3%; $P > 0.1$; Fig. 6ab). Similarly, warming increased R_a/GPP (+12%; $P < 0.1$) but decreased Residual/GPP (-15%; $P < 0.05$) prior to the drought (Figs 6-7). Thus, experimental warming increased the partitioning of GPP to aboveground components (Fig. 7a-b) and decreased partitioning belowground (Fig. 7c). The experimental drought had weak effects on partitioning, none of which were statistically significant ($P > 0.1$).

Growth and maintenance respiration

We combined growth and respiratory measurements to infer changes in respiratory C efflux attributable to growth versus maintenance respiration (Amthor, 2000). There was a strong and linear relationship between R_a per unit aboveground tree C and relative growth rate (RGR; Fig. 8). Neither the slope nor the intercept of this relationship were affected by experimental treatments (all $P > 0.1$). Thus, we present a common relationship across all measurements. The y-intercept of this relationship was positive (mean of 0.0213, 95% CI of 0.0157 to 0.0268), indicating significant R_a in the absence of aboveground growth, reflecting maintenance respiration. The lack of a warming effect on this y-intercept is consistent with respiratory temperature acclimation; trees in the ambient and warmed treatments expended similar amounts of C on maintenance respiration, despite the increased temperature in the warmed treatment. The slope of the relationship (Fig. 8) was strongly positive (mean of 0.0059, 95% CI of 0.0053 to 0.0065), indicating that much of the R_a observed at the crown scale was attributable to construction respiration. Observations during the drought period followed the general relationship, with lower values on both axes (Fig. 8). Thus, the experimental drought reduced R_a primarily via a reduction in growth respiration.

We also directly estimated coefficients for growth and maintenance respiration by fitting equation 2 to the fortnightly dataset of standing biomass, growth rate, and respiration. We estimate the growth respiration to consume approximately 0.3 gC per gram of biomass C produced, and maintenance respiration to consume approximately 0.015 gC per g of standing biomass C per day (Table 1). These coefficients did not differ across the ambient and warmed treatment ($P > 0.3$).

Discussion

Summary

We studied the experimental effects of warming and drought on the C allocation of *Eucalyptus tereticornis* trees using a combination of growth and whole-crown flux measurements. Experimental warming increased the proportion of GPP that was allocated to aboveground uses and decreased the proportion of GPP that was allocated belowground. This was consistent with a reduced root mass fraction in the warmed treatments at the final harvest. The experimental drought reduced CO_2 and H_2O fluxes but did not affect the allocation of C, perhaps because tree access to deep soil water prevented them from experiencing strongly negative water potentials. There were no interactions between warming and drought on C partitioning terms, so we discuss the impacts of warming and drought separately.

Effects of experimental warming on C allocation

Experimental warming strongly affected several aspects of tree C allocation. Warming increased the fractional partitioning of GPP to aboveground uses, including growth and respiration, at the expense of C partitioning belowground. This observation is consistent with some soil warming experiments (e.g., Melillo *et al*., 2002, 2011) that attributed this effect to a warming-induced stimulation of soil nutrient availability. However, it is also possible that experimental warming directly stimulated the activity of meristems aboveground, such that a smaller remainder of fixed C was available for transport and use belowground. Such a mechanism would imply an aboveground priority in tree C allocation, consistent with previous work on forest C budgets and elevated atmospheric CO_2 treatments (Palmroth *et al.*, 2006). This mechanism also makes sense given the structural arrangement of tree phloem, as aboveground tissues have the opportunity to remove sucrose from the phloem before belowground tissues (Lemoine *et al.*, 2013; Furze *et al.*, 2018). The mechanisms regarding soil nutrient availability and aboveground metabolic activity are not mutually exclusive. For example, enhanced N supply from soil N mineralization may have enabled the increased aboveground metabolism in the warmed treatment, which may have resulted in the larger consumption of GPP aboveground in the warmed relative to the ambient treatment.

We also acknowledge that warming may have influenced allocation indirectly via ontogenetic drift. A meta-analysis documented a decline in root to shoot ratios as trees grew larger, possibly reflecting an ontogenetic effect on belowground allocation (Mokany *et al.*, 2006), although we hesitate to infer allocation directly from root to shoot ratios (Reich, 2002; Litton *et al.*, 2007). In this experiment, the allocation terms (e.g., NPP_a/GPP, R_a/GPP, and residual/GPP) were not significantly correlated with any metric of tree size, suggesting that the warming effect is unlikely to reflect ontogeny.

We previously demonstrated that aboveground autotrophic respiration acclimated nearly homeostatically to experimental warming in this experiment, both at the leaf-scale (Aspinwall *et al.*, 2016) and at the whole-crown scale (Drake *et al.*, 2016b). As such, the demonstration that warming increased R_a (Fig. 5) may appear contradictory. We emphasize that our previous presentations of autotrophic respiration were expressed per unit leaf area (Drake *et al.*, 2016b; Aspinwall *et al.*, 2016), while the current study shows the total fluxes per tree (Fig. 5c). Experimental warming increased R_a primarily by increasing growth and tree size early in the experiment. Furthermore, the common relationship between relative growth rate and R_a per unit tree mass for the ambient and warmed treatment is indicative of homeostatic acclimation of maintenance respiration in this experiment (Fig. 8). The stimulation of whole-crown R_a by warming was primarily attributable to an increase in respiration to support growth. Thus, we suggest that this study is in agreement with previous published work from this experiment (Drake *et al.*, 2016b; Aspinwall *et al.*, 2016), where homeostatic acclimation of respiration to experimental warming prevented a warming-induced increase in maintenance respiration, while a warming effect on growth stimulated growth respiration and increased whole-crown R_a.

The increased allocation of C aboveground in the warmed treatment, combined with homeostatic acclimation of maintenance respiration, likely contributed to the observed warming-induced stimulation in growth during the first half of this experiment (Fig. 1). Experimental warming had neutral or negative effects on leaf-level photosynthetic rates in this study (Drake *et al.*, 2016b; Aspinwall *et al.*, 2016), so a warming-induced stimulation of growth was somewhat surprising. We suggest that an increase in C partitioning aboveground (Fig. 6a) was associated with accelerated leaf development early in the experiment in these young and rapidly growing trees (Fig. 1c), such that trees exposed to the warmed treatment had higher rates of crown-scale photosynthesis (Fig. 5a) primarily through a warming effect on total crown leaf area. That is, the warmed treatment got a head start in leaf area production, which compounded over time. This is consistent with nutrient fertilization studies, in which increases in leaf area rather than changes in leaf N or leaf function, often dominates the growth responses of rapidly growing plants (Sinclair & Horie, 1989; Gastal & Lemaire, 2002; Lovelock *et al.*, 2004; Wang *et al.*, 2012), although there are exceptions (Santiago *et al.*, 2012). This is also consistent with other experimental manipulations, in which a stimulation of leaf area development early in an experiment can strongly affect exponential growth trajectories (Tjoelker *et al.*, 1998; Kirschbaum, 2011; Drake *et al.*, 2017).

Effects of drought on C allocation

We did not detect any significant effects of drought on C partitioning. The drought appeared to reduce all C fluxes proportionally, such that the ratios of C fluxes to GPP was unchanged. We recognize

that our ability to resolve C partitioning belowground was limited by the nature of the measurements based on the residual, and our lack of root biomass measurements through time. The biomass in roots relative to the total at the harvest (root mass ratio; Fig 3b) did indicate an interactive effect of drought and warming, possibly via small differences in the partitioning of GPP to roots that accumulated over time. Perhaps the ambient temperature trees had sufficient carbohydrate reserves to fuel additional root growth in the drought treatment, while warmed temperature trees were consuming more carbohydrates aboveground and were thus unable to increase root growth in the drought. This speculative process may explain the observed interaction between warming and drought on root mass ratio (Fig. 3b).

Trees acquired water from deep in the soil profile during the drought. Leaf predawn water potential declined to only approximately -0.5 MPa, which is a moderate value that is not indicative of pronounced water stress. Previous studies have shown that groundwater use enables vegetation to avoid production declines under conditions of surface moisture limitation (Baldocchi *et al.*, 2010; Barbeta *et al.*, 2015), and several eucalypt species are well-known users of groundwater (Mensforth *et al.*, 1994; Pfautsch *et al.*, 2011, 2015; Eamus *et al.*, 2015; Zolfaghar *et al.*, 2017). Furthermore, Koirala *et al.* (2017) demonstrated correlations between GPP and groundwater table depth that were present over approximately 70% of the vegetated surface of the earth, suggesting that vegetation-groundwater interactions are common and globally relevant. Our study demonstrates that some trees may utilize access to soil water at depth to maintain moderate rates of photosynthetic C uptake and growth during extended droughts that lead to dry surface soils.

Implications for mathematical models

Many ecosystem and earth system models begin their simulation of ecosystem C cycling by predicting GPP as a function of leaf area and environmental drivers. GPP is then partitioned into component terms including R_a and the production of leaf, wood, and root mass. Our observations suggest that tree C allocation of GPP to these terms can be influenced by environmental drivers such as temperature. That is, the observations presented here are not consistent with static partitioning schemes with fixed and constant partitioning of GPP into component fluxes. However when aggregated over longer time periods, our average partitioning coefficients (approximately 30% of GPP to aboveground respiration, 43% of GPP to aboveground growth, and 27% to belowground fluxes) are comparable with values used in some ecosystem models (De Kauwe *et al.*, 2014). The observations presented here are also not consistent with a dynamic C partitioning scheme based on Sprengel and Leibig's law of the minimum (van der Ploeg *et al.*, 1999), where C would be preferentially allocated to increase the acquisition of the factor most limiting primary production. Furthermore, Aspinwall *et al.* (2016) recently documented strong seasonal variation in carbohydrate storage in these evergreen trees, characterized by the buildup of high starch

concentrations during the winter and a drawdown of these reserves during the summer. It appears that these trees partially utilize a non-structural carbohydrate storage reserve to fuel growth and metabolism during the hot summer. Based on these observations, we suggest that a dynamic allocation scheme incorporating a dynamic carbohydrate reserve may be appropriate for future investigation (e.g., Fatichi *et al.*, 2014; Pugh *et al.*, 2016).

Conclusions

We used detailed measurements of growth and whole-crown flux measurements to study the effects of warming and drought on the C allocation of *Eucalyptus tereticornis* trees. Experimental warming increased the proportion of GPP that was allocated to aboveground uses and decreased the proportion of GPP that was allocated belowground. Such a change in tree C allocation may have important implications for tree growth, forest C storage, and soil nutrient cycling in a warmer world. In particular, increased allocation aboveground in a warmer world may stimulate leaf area development and aboveground growth during conditions of sufficient soil resource supply.

Acknowledgements

We thank Burhan Amiji (Western Sydney University) for maintaining the site, for collecting much of the growth and harvest data, and for his excellent research support. This experiment was made possible through a collaboration with Sune Linder and the Swedish University of Agricultural Sciences, who designed, built, and generously provided the whole tree chambers. We also gratefully acknowledge Courtney Campany (Colgate University) for his measurements of fine root biomass as well as Renee Smith, Carrie Drake (Western Sydney University), and Richard Harwood (Sydney University) for their help with the whole-tree harvests. This research was supported by the Australian Research Council (Discovery, DP140103415), a New South Wales government Climate Action Grant (NSW T07/CAG/016), the Hawkesbury Institute for the Environment, and Western Sydney University.

Authorship statement

JED co-led the experimental design, contributed to data collection for the chamber flux, and led the data analysis, modeling, and writing. MGT was the senior scientific lead; he co-led the experimental design and made large contributions to analysis, interpretation, and writing. MJA contributed to the experimental design, data collection and interpretation, and writing. PBR contributed to the experimental design, interpretation, and writing. SP contributed to experimental design, data collection and interpretation, and writing. CVMB contributed to the

measurements of chamber flux, and contributed to experimental design, data analysis, and writing.

Table 1. Estimate of aboveground growth and maintenance respiration coefficients derived from equation 2, with standard errors (SE), and 95% confidence intervals; parameters were statistically equivalent across ambient and warmed treatments (all $P > 0.3$).

Term	Units	Ambient		Warmed	
		Mean (SE)	95% CI	Mean (SE)	95% CI
g_r (growth respiration rate)	g C respired per g C growth	0.32 (0.02)	0.27-0.37	0.28 (0.03)	0.21-0.36
m_r (maintenance respiration rate)	g C respired per g C standing aboveground biomass per day	0.015 (0.001)	0.012-0.019	0.017 (0.002)	0.013-0.021

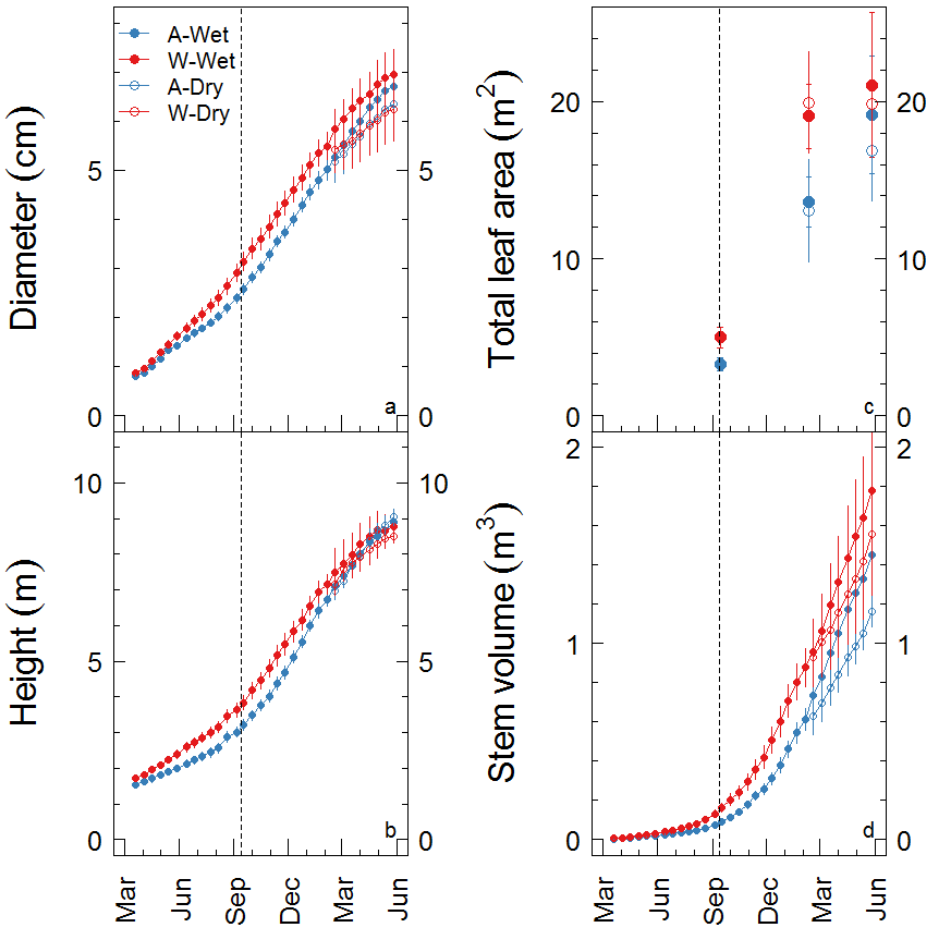

Figure 1. Growth of *Eucalyptus tereticornis* trees exposed to warming and drought. Trees were either exposed to ambient T_{air} ("A", blue) or warming of +3 ºC ("W", red), and either well-watered ("Wet", solid points) or drought conditions ("Dry", open points). Stem diameter (a) was measured at 65-cm height, and height reflects total stem length (b). Total leaf area was directly measured on three dates (c) and stem volume was calculated from diameter measurements along the stem of each tree (d). The vertical dashed line denotes when CO_2 and H_2O flux measurements began. Points reflect the mean, error bars denote 1SEM (n = 6 until Feb 2014, when the drought treatment began and n = 3).

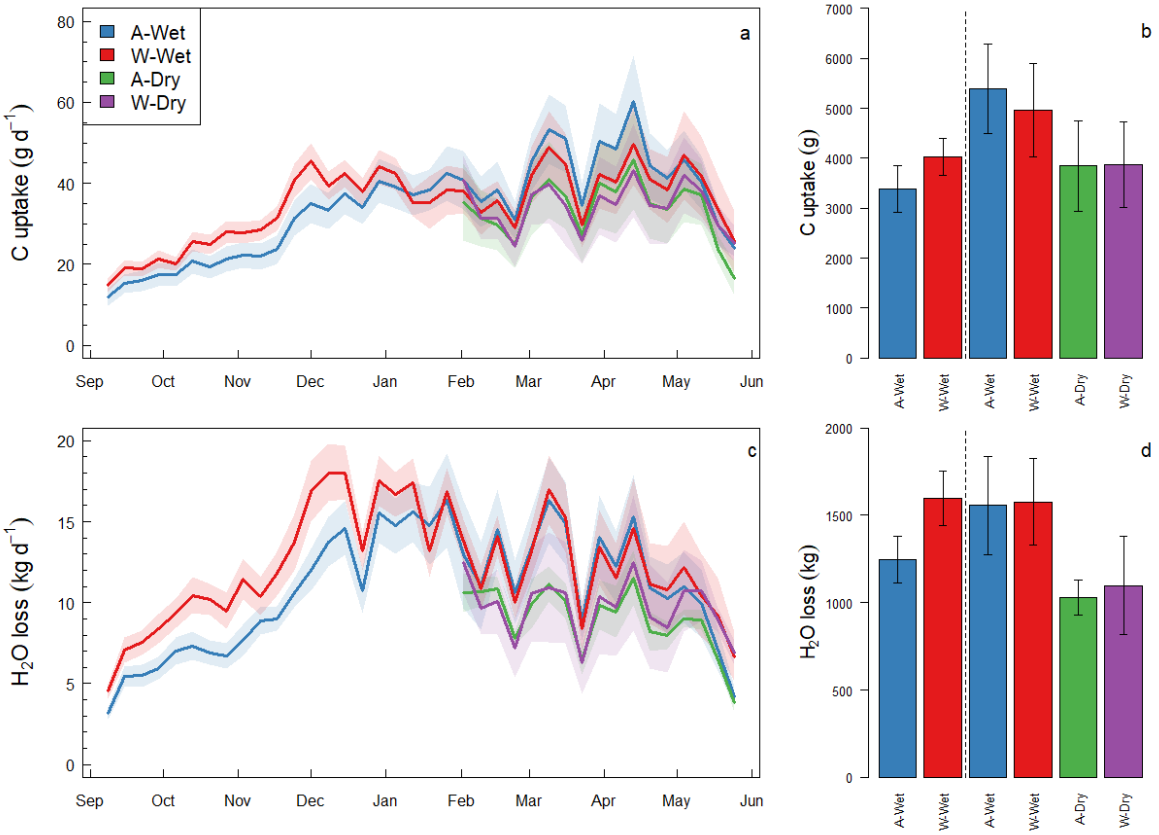

Figure 2. Summary of measured CO_2 and H_2O fluxes for twelve *Eucalyptus tereticornis* trees exposed to ambient (A) or warmed (W) air temperatures in 2013 and 2014. All trees were maintained in well-water conditions (Wet) until mid-Feb, when half of the trees were subjected to a soil drydown (Dry). We show weekly averages of the measured daily net C uptake (a) and the sum of net C uptake for the two measurement periods (pre-drought, drought; b). We also show weekly averages of the measured daily net H_2O loss to transpiration (c) and the H_2O loss to transpiration summed across the two measurement periods (d). In (a) and (c), lines reflect the mean and shaded areas reflect the standard error. The dotted vertical lines in (b) and (d) separate the pre-drought (left) and drought periods (right). These plots reflect >580,000 individual flux measurements at 15-minute resolution.

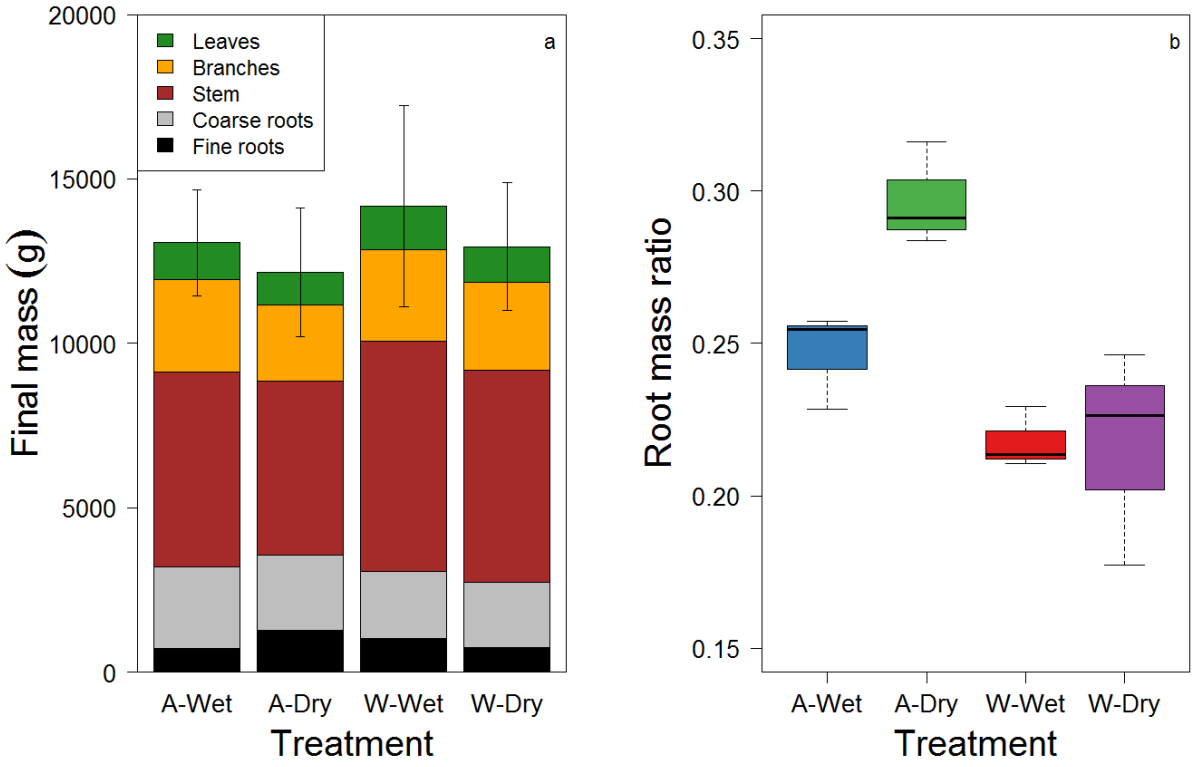

Figure 3. Biomass components at final harvest for twelve *Eucalyptus tereticornis* trees exposed to ambient (A) or warmed (W) air temperatures and either well-watered conditions (Wet) or a soil drydown treatment (Dry). Note that these data reflect grams of dry mass. Each of the measured biomass components (a) reflects the mean of three trees per treatment, the error bars reflect the standard error of the total measured mass. The root mass ratio (b) reflects the sum of coarse and fine roots relative to total tree mass. Warming reduced the root mass ratio, while the drought treatment increased root mass ratio in the ambient temperature treatment only. The root mass ratio interaction primarily follows the response of fine roots, although stem wood and coarse roots also contributed.

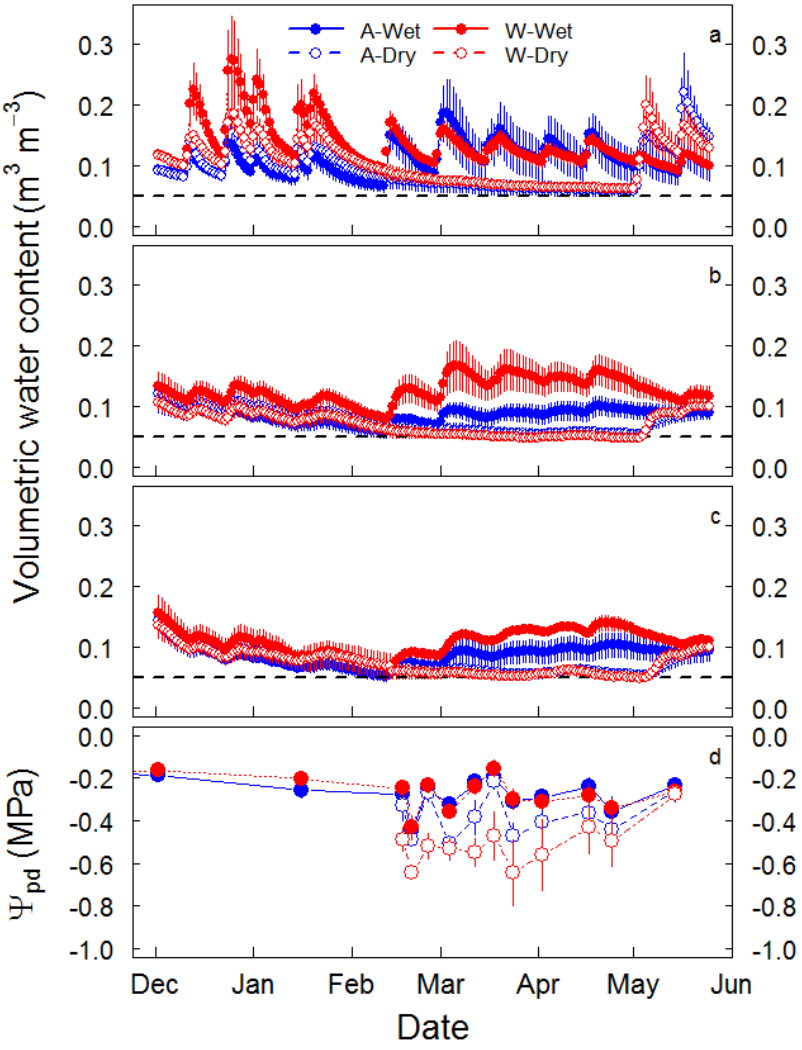

538

539 **Figure 4**. Soil volumetric water content and predawn leaf water potential (Ψ_{pd}) for twelve *Eucalyptus*
540 *tereticornis* trees exposed to ambient (A) or warmed (W) air temperatures. All trees were maintained in
541 well-water conditions (Wet) until mid-Feb, when half of the trees were subjected to a soil drydown (Dry).
542 We show daily averages of the measured volumetric water content in surface soils (~0.1-m-depth; a), an
543 intermediate depth (~0.5-m-depth; b), and in deep soils just above the hard layer of partially cemented
544 manganese nodules (~1-m-depth; c). We also show leaf Ψ_{pd} measured throughout the drydown (d). Points
545 reflect the mean and error bars reflect the standard error (n = 6 or 3). Note that Ψ_{pd} was moderate in all
546 treatments.

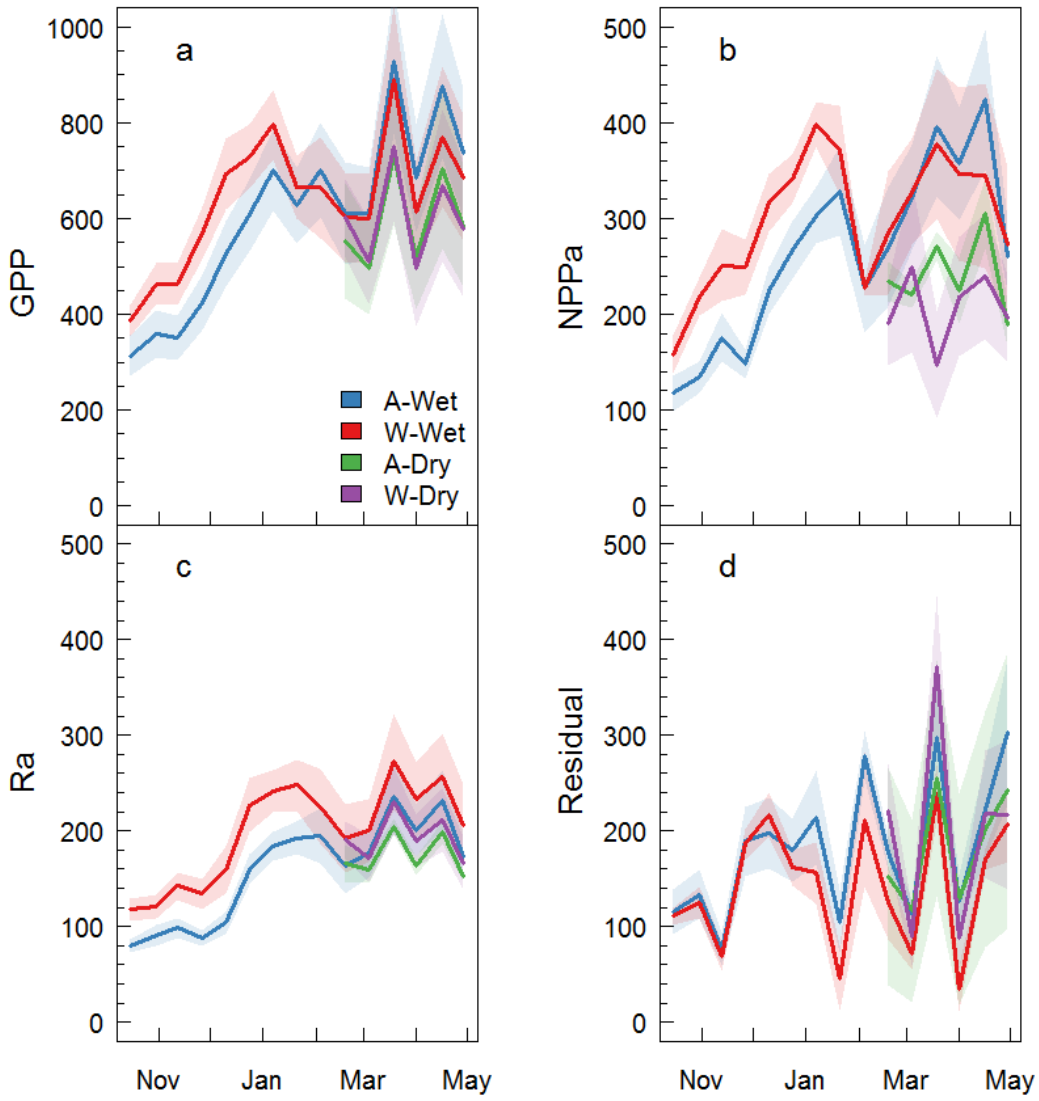

Figure 5. Fortnightly C fluxes for twelve *Eucalyptus tereticornis* trees exposed to ambient (A) or warmed (W) air temperatures. All fluxes are presented in units of g C tree^{-1} fortnight^{-1}. All trees were maintained in well-water conditions until mid-Feb (Wet), when half of the trees were subjected to a soil drydown (Dry). Solid lines reflect the mean of fortnightly data (i.e., two-weekly) and shaded areas reflect 1SEM. Measurements include gross primary production (GPP; a), aboveground net primary production (NPP_a; b), aboveground autotrophic respiration (R_a; c), and the residual (d). The residual reflects belowground C flux and measurement error. Note that the y-axis scale is twice as large for GPP relative to the other fluxes.

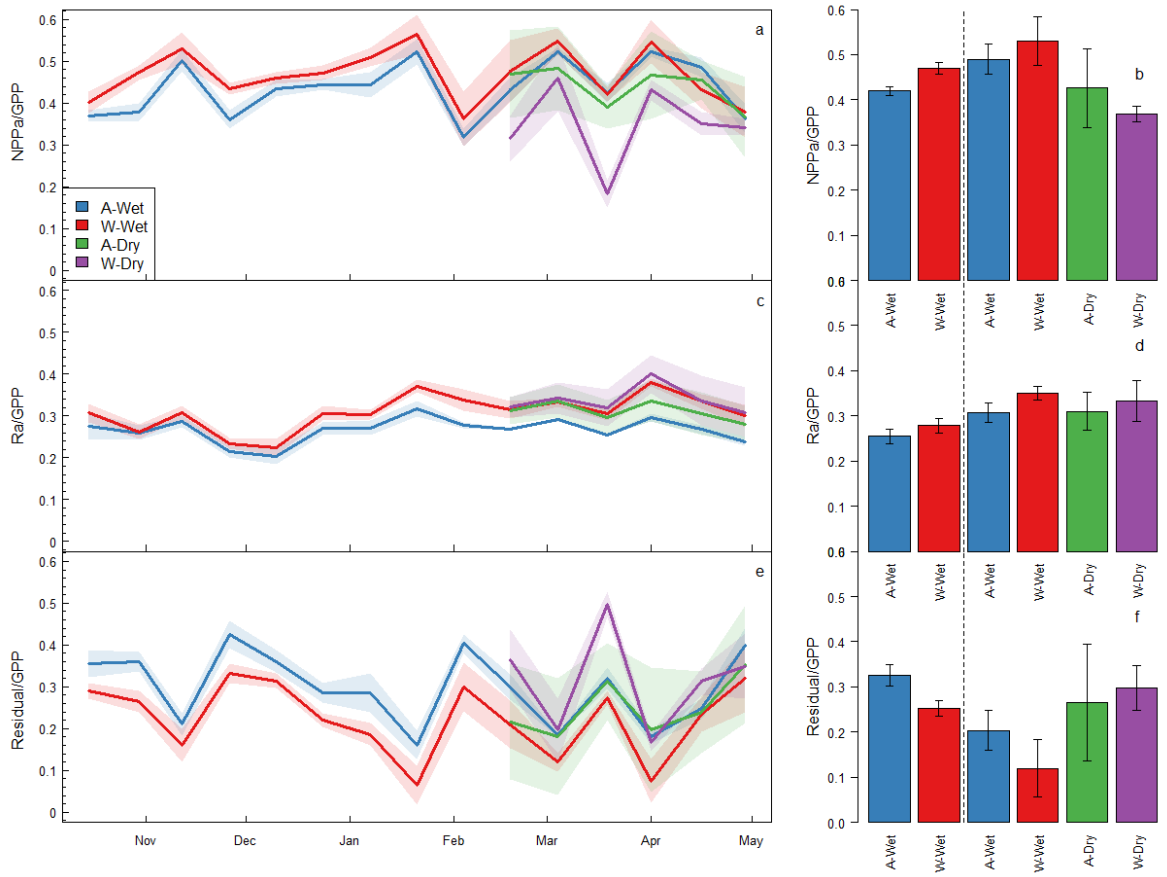

Figure 6. The fractional partitioning of gross primary production (GPP) for twelve *Eucalyptus tereticornis* trees. GPP was partitioned into aboveground net primary production (NPP_a; a-b), aboveground autotrophic respiration (R_a; c-d), and the residual C, which includes belowground C allocation and measurement error (e-f). All trees were maintained in well-water conditions (Wet) until mid-Jan, when half of the trees were subjected to a soil drydown (Dry). Bar charts of flux partitioning terms (b, d, f) represent the mean (±1SEM), and the dotted vertical lines separate the pre-drought (left) and drought periods (right).

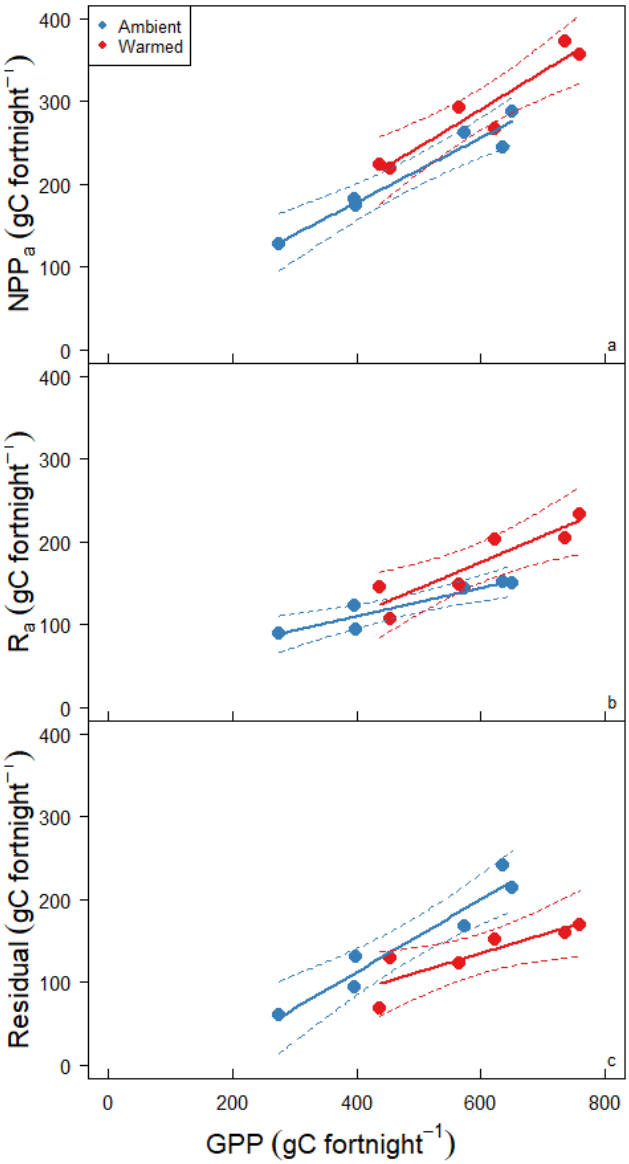

564

565 **Figure 7**. The fractional partitioning of gross primary production (GPP) for twelve *Eucalyptus*
566 *tereticornis* trees grown under ambient and elevated temperature. Data for each tree were averaged across
567 the pre-drought period; each point reflects an individual tree (n = 6). GPP was partitioned into
568 aboveground net primary production (NPP_a; a), aboveground autotrophic respiration (R_a; b), and the
569 residual C, which includes belowground C allocation (c). Solid lines reflect linear models fit to each
570 treatment; dashed lines reflect the 95% confidence interval.

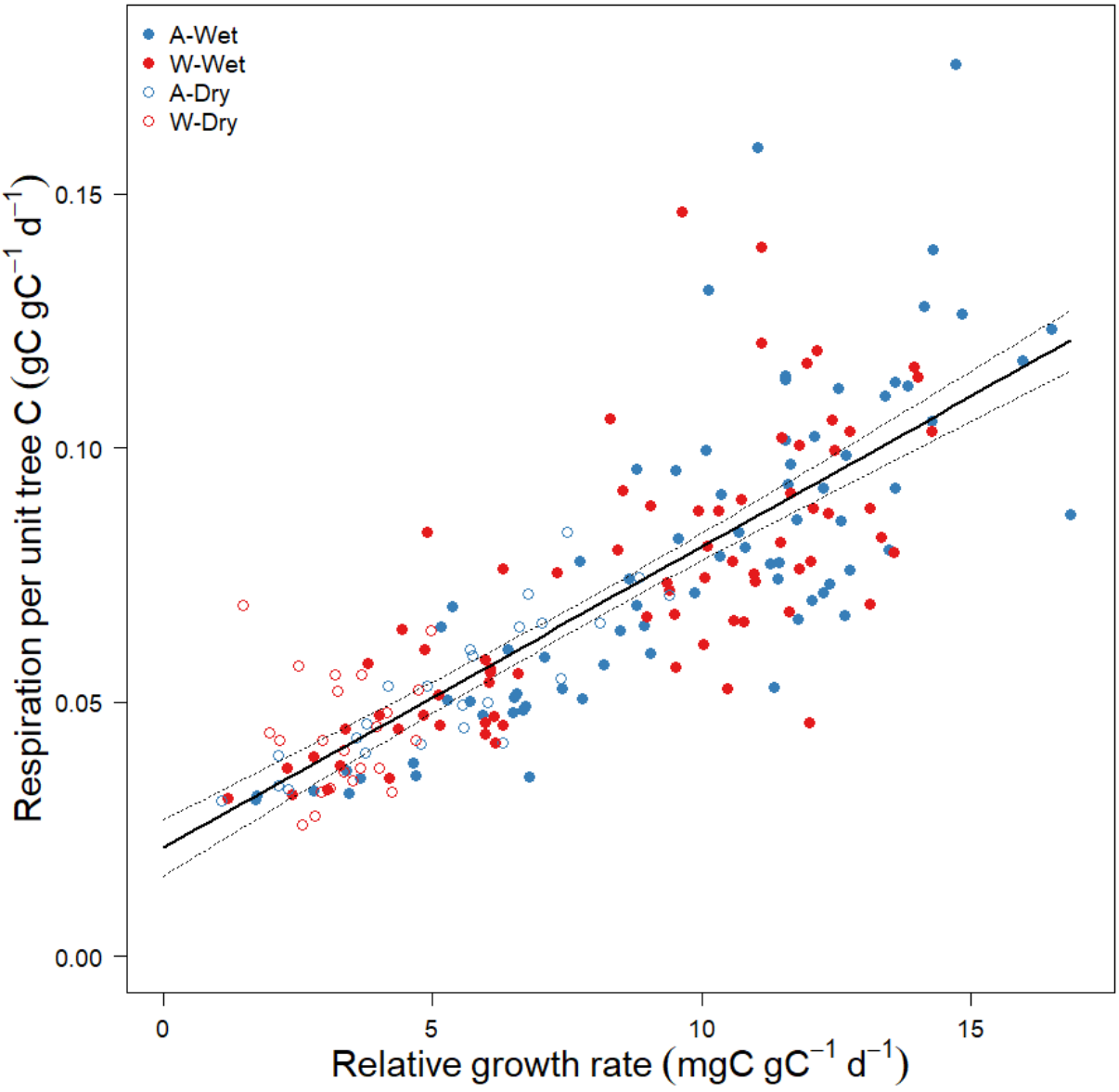

Figure 8. Partitioning of aboveground respiration into maintenance and growth components. Each point reflects a tree during a fortnightly growth interval. Note that the y-intercept reflects the maintenance respiration component and the slope reflects the growth respiration component. Neither the slope nor the intercept were affected by experiment treatments (mixed effects model with random intercepts for each chamber, $P > 0.5$). The solid lines reflects models fit to the ambient temperature (A) and warmed temperature (W) data and dashed lines reflect the 95% confidence interval. All of the data were well-described by a single linear function ($Y = 0.021 + 0.0059x$, $r^2 = 0.64$, $P < 0.001$; *not shown*).

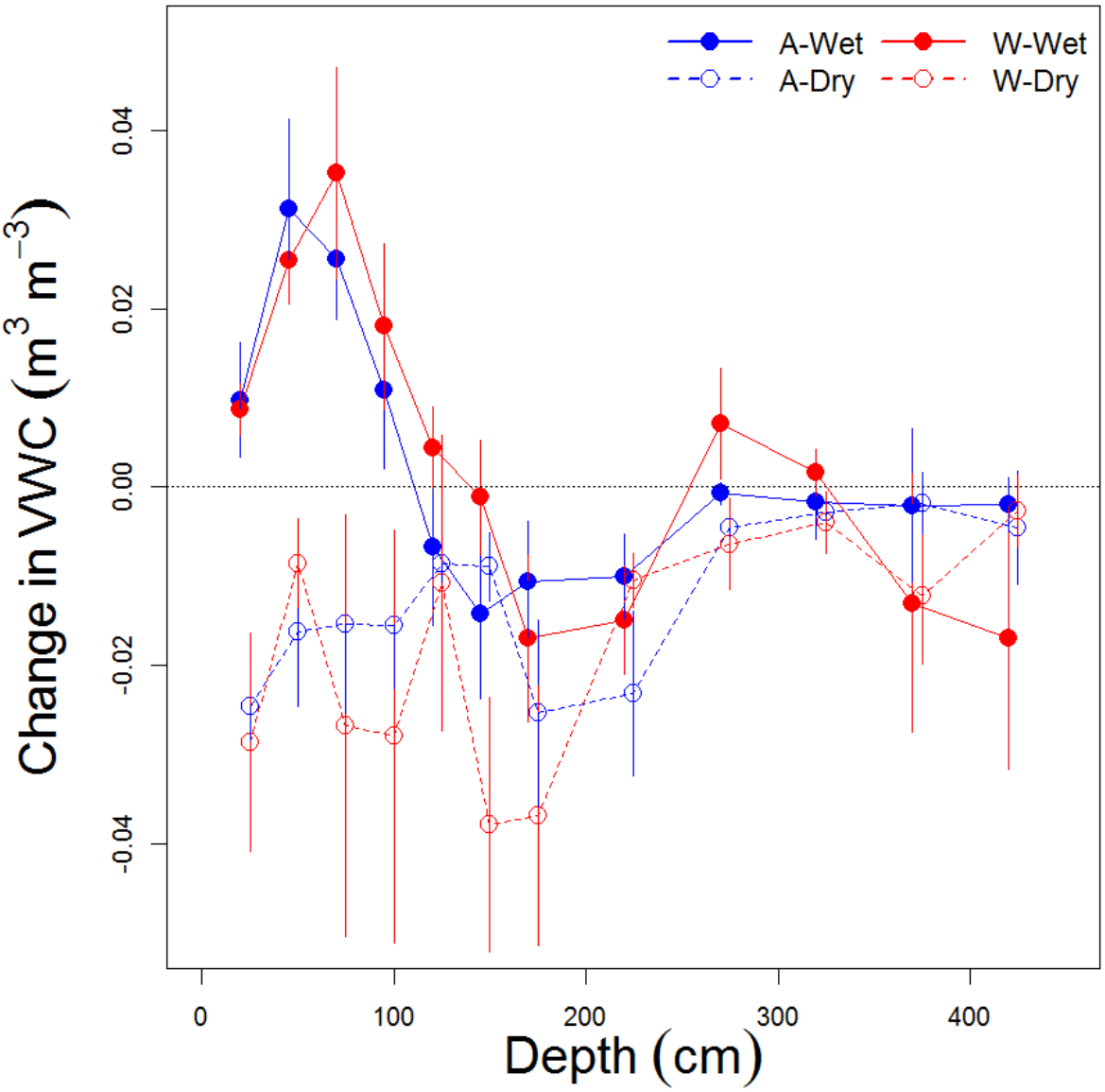

Figure S1. The change in volumetric water content (VWC) throughout the soil profile, comparing the end of the drought to the beginning of the drought. VWC was measured with the neutron probe method; negative values reflect reductions in VWC from the beginning (17 Feb 2014) to the end of the drought (24 April 2014). Points reflect means and error bars reflect 1SEM (n = 3). Note that trees in the dry treatment likely acquired water from soils as deep as 200 cm during the drought. The positive values in the shallow soils of "Wet" trees reflects the addition of H_2O via surface irrigation.

References

Adu-Bredu S, Hagihara A. **2003**. Long-term carbon budget of the above-ground parts of a young hinoki cypress (Chamaecyparis obtusa) stand. *Ecological Research* **18**: 165–175.

Allen CD, Breshears DD, McDowell NG. **2015**. On underestimation of global vulnerability to tree mortality and forest die-off from hotter drought in the Anthropocene. *Ecosphere* **6**: 129.

Amthor JS. **2000**. The McCree–de Wit–Penning de Vries–Thornley Respiration Paradigms: 30 Years Later. *Annals of Botany* **86**: 1–20.

Aspinwall MJ, Drake JE, Campany C, Varhammar A, Ghannoum O, Tissue DT, Reich PB, Tjoelker MG. **2016**. Convergent acclimation of leaf photosynthesis and respiration to prevailing ambient temperatures under current and warmer climates in Eucalyptus tereticornis. *New Phytologist* **212**: 354–367.

Atkin OK, Tjoelker MG. **2003**. Thermal acclimation and the dynamic response of plant respiration to temperature. *Trends in Plant Science* **8**: 343–351.

Baldocchi DD, Ma S, Rambal S, Misson L, Ourcival J-M, Limousin J-M, Pereira J, Papale D. **2010**. On the differential advantages of evergreenness and deciduousness in mediterranean oak woodlands: a flux perspective. *Ecological Applications* **20**: 1583–1597.

Barbeta A, Mejía-Chang M, Ogaya R, Voltas J, Dawson TE, Peñuelas J. **2015**. The combined effects of a long-term experimental drought and an extreme drought on the use of plant-water sources in a Mediterranean forest. *Global Change Biology* **21**: 1213–1225.

Barton CVM, Duursma RA, Medlyn BE, Ellsworth DS, Eamus D, Tissue DT, Adams MA, Conroy J, Crous KY, Liberloo M, *et al.* 2012. Effects of elevated atmospheric [CO2] on instantaneous transpiration efficiency at leaf and canopy scales in Eucalyptus saligna. *Global Change Biology* **18**: 585–595.

Barton CVM, Ellsworth DS, Medlyn BE, Duursma RA, Tissue DT, Adams MA, Eamus D, Conroy JP, McMurtrie RE, Parsby J, *et al.* 2010. Whole-tree chambers for elevated atmospheric CO2 experimentation and tree scale flux measurements in south-eastern Australia: The Hawkesbury Forest Experiment. *Agricultural and Forest Meteorology* **150**: 941–951.

Blessing CH, Werner RA, Siegwolf R, Buchmann N. **2015**. Allocation dynamics of recently fixed carbon in beech saplings in response to increased temperatures and drought. *Tree Physiology* **35**: 585–598.

Burke EJ, Brown SJ, Christidis N. **2006**. Modeling the Recent Evolution of Global Drought and Projections for the Twenty-First Century with the Hadley Centre Climate Model. *Journal of Hydrometeorology* **7**: 1113–1125.

De Kauwe MG, Medlyn BE, Zaehle S, Walker AP, Dietze MC, Wang Y-P, Luo Y, Jain AK, El-Masri B, Hickler T, *et al.* 2014. Where does the carbon go? A model–data intercomparison of vegetation carbon allocation and turnover processes at two temperate forest free-air CO2 enrichment sites. *New Phytologist* **203**: 883–899.

DeLucia EH, Moore DJ, Norby RJ. **2005**. Contrasting responses of forest ecosystems to rising atmospheric CO2: Implications for the global C cycle. *Global Biogeochemical Cycles* **19**: GB3006.

Dietze MC, Sala A, Carbone MS, Czimczik CI, Mantooth JA, Richardson AD, Vargas R. **2014**. Nonstructural Carbon in Woody Plants. *Annual Review of Plant Biology* **65**: 667–687.

Doughty CE, Malhi Y, Araujo-Murakami A, Metcalfe DB, Silva-Espejo JE, Arroyo L, Heredia JP, Pardo-Toledo E, Mendizabal LM, Rojas-Landivar VD, *et al.* 2014. Allocation trade-offs dominate the response of tropical forest growth to seasonal and interannual drought. *Ecology* **95**: 2192–2201.

Doughty CE, Metcalfe D, Girardin C a. J, Farfan Amezquita F, Galiano Cabrera D, Huaraca Huasco W, Silva-Espejo JE, Araujo-Murakami A, Costa D, C M, *et al.* 2015. Drought impact on forest carbon dynamics and fluxes in Amazonia. *Nature* **519**: 78–140.

Drake JE, Aspinwall MJ, Pfautsch S, Rymer PD, Reich PB, Smith RA, Crous KY, Tissue DT, Ghannoum O, Tjoelker MG. **2015**. The capacity to cope with climate warming declines from temperate to tropical latitudes in two widely distributed Eucalyptus species. *Global Change Biology* **21**: 459–472.

Drake JE, Gallet-Budynek A, Hofmockel KS, Bernhardt ES, Billings SA, Jackson RB, Johnsen KS, Lichter J, McCarthy HR, McCormack ML, *et al.* 2011. Increases in the flux of carbon belowground stimulate nitrogen uptake and sustain the long-term enhancement of forest productivity under elevated CO2. *Ecology Letters* **14**: 349–357.

Drake J, Tjoelker M, Aspinwall MJ. **2016a**. Drake_NewPhyt_2016_WTC3_RtoGPP_forfigshare.zip.

Drake JE, Tjoelker MG, Aspinwall MJ, Reich PB, Barton CVM, Medlyn BE, Duursma RA. **2016b**. Does physiological acclimation to climate warming stabilize the ratio of canopy respiration to photosynthesis? *New Phytologist* **211**: 850–863.

Drake JE, Vårhammar A, Kumarathunge D, Medlyn BE, Pfautsch S, Reich PB, Tissue DT, Ghannoum O, Tjoelker MG. **2017**. A common thermal niche among geographically diverse populations of the widely distributed tree species Eucalyptus tereticornis: No evidence for adaptation to climate-of-origin. *Global Change Biology* **23**: 5069–5082.

Duursma RA, Barton CVM, Eamus D, Medlyn BE, Ellsworth DS, Forster MA, Tissue DT, Linder S, McMurtrie RE. **2011**. Rooting depth explains [CO2] x drought interaction in Eucalyptus saligna. *Tree Physiology* **31**: 922–931.

Duursma RA, Barton CVM, Lin Y-S, Medlyn BE, Eamus D, Tissue DT, Ellsworth DS, McMurtrie RE. **2014**. The peaked response of transpiration rate to vapour pressure deficit in field conditions can be explained by the temperature optimum of photosynthesis. *Agricultural and Forest Meteorology* **189**: 2–10.

Duursma RA, Falster DS. **2016**. Leaf mass per area, not total leaf area, drives differences in above-ground biomass distribution among woody plant functional types. *New Phytologist* **212**: 368–376.

Eamus D, Zolfaghar S, Villalobos-Vega R, Cleverly J, Huete A. **2015**. Groundwater-dependent ecosystems: recent insights from satellite and field-based studies. *Hydrol. Earth Syst. Sci.* **19**: 4229–4256.

Edler B, Buerger J, Breitsameter L, Steinmann H-H, Isselstein J. **2015**. Growth responses to elevated temperature and reduced soil moisture during early establishment of three annual weeds in four soil types. *Journal of Plant Diseases and Protection* **122**: 39–48.

Epron D, Bahn M, Derrien D, Lattanzi FA, Pumpanen J, Gessler A, Högberg P, Maillard P, Dannoura M, Gérant D, *et al.* 2012. Pulse-labelling trees to study carbon allocation dynamics: a review of methods, current knowledge and future prospects. *Tree Physiology* **32**: 776–798.

Farooq M, Wahid A, Kobayashi N, Fujita D, Basra SMA. **2009**. Plant drought stress: effects, mechanisms and management. *Agronomy for Sustainable Development* **29**: 185–212.

Fatichi S, Leuzinger S, Koerner C. **2014**. Moving beyond photosynthesis: from carbon source to sink-driven vegetation modeling. *New Phytologist* **201**: 1086–1095.

Feng L, Reffye P de, Dreyfus P, Auclair D. **2012**. Connecting an architectural plant model to a forest stand dynamics model—application to Austrian black pine stand visualization. *Annals of Forest Science* **69**: 245–255.

Finzi AC, Abramoff RZ, Spiller KS, Brzostek ER, Darby BA, Kramer MA, Phillips RP. **2015**. Rhizosphere processes are quantitatively important components of terrestrial carbon and nutrient cycles. *Global Change Biology* **21**: 2082–2094.

Franklin O, Johansson J, Dewar RC, Dieckmann U, McMurtrie RE, Brännström Å, Dybzinski R. **2012**. Modeling carbon allocation in trees: a search for principles. *Tree Physiology* **32**: 648–666.

Friedlingstein P, Joel G, Field CB, Fung IY. **1999**. Toward an allocation scheme for global terrestrial carbon models. *Global Change Biology* **5**: 755–770.

Furze ME, Trumbore S, Hartmann H. **2018**. Detours on the phloem sugar highway: stem carbon storage and remobilization. *Current Opinion in Plant Biology* **43**: 89–95.

Gastal F, Lemaire G. **2002**. N uptake and distribution in crops: an agronomical and ecophysiological perspective. *Journal of Experimental Botany* **53**: 789–799.

Gower ST, Krankina O, Olson RJ, Apps M, Linder S, Wang C. **2001**. Net primary production and carbon allocation patterns of boreal ecosystems. *Ecological Applications* **11**: 1395–1411.

Hartmann H, McDowell NG, Trumbore S. **2015**. Allocation to carbon storage pools in Norway spruce saplings under drought and low CO2. *Tree Physiology* **35**: 243–252.

Högberg P, Nordgren A, Buchmann N, Taylor AF, Ekblad A, Högberg MN, Nyberg G, Ottosson-Löfvenius M, Read DJ. **2001**. Large-scale forest girdling shows that current photosynthesis drives soil respiration. *Nature* **411**: 789–792.

Hommel R, Siegwolf R, Zavadlav S, Arend M, Schaub M, Galiano L, Haeni M, Kayler ZE, Gessler A. **2016**. Impact of interspecific competition and drought on the allocation of new assimilates in trees. *Plant Biology* **18**: 785–796.

Kirschbaum MUF. **2011**. Does Enhanced Photosynthesis Enhance Growth? Lessons Learned from CO2 Enrichment Studies. *Plant Physiology* **155**: 117–124.

Koirala S, Jung M, Reichstein M, de Graaf IEM, Camps-Valls G, Ichii K, Papale D, Ráduly B, Schwalm CR, Tramontana G, *et al.* 2017. Global distribution of groundwater-vegetation spatial covariation. *Geophysical Research Letters* **44**: 2017GL072885.

Kuster TM, Arend M, Bleuler P, Günthardt-Goerg MS, Schulin R. **2013**. Water regime and growth of young oak stands subjected to air-warming and drought on two different forest soils in a model ecosystem experiment. *Plant Biology* **15**: 138–147.

Landsberg JJ, Waring RH. **1997**. A generalised model of forest productivity using simplified concepts of radiation-use efficiency, carbon balance and partitioning. *Forest Ecology and Management* **95**: 209–228.

Lemoine R, La Camera S, Atanassova R, Dedaldechamp F, Allario T, Pourtau N, Bonnemain J-L, Laloi M, Coutos-Thevenot P, Maurousset L, *et al.* 2013. Source-to-sink transport of sugar and regulation by environmental factors. *Frontiers in Plant Science* **4**: 272.

Leon-Sanchez L, Nicolas E, Nortes PA, Maestre FT, Querejeta JI. **2016**. Photosynthesis and growth reduction with warming are driven by nonstomatal limitations in a Mediterranean semi-arid shrub. *Ecology and Evolution* **6**: 2725–2738.

Litton CM, Raich JW, Ryan MG. **2007**. Carbon allocation in forest ecosystems. *Global Change Biology* **13**: 2089–2109.

Lovelock CE, Feller IC, Mckee KL, Engelbrecht BMJ, Ball MC. **2004**. The effect of nutrient enrichment on growth, photosynthesis and hydraulic conductance of dwarf mangroves in Panama. *Functional Ecology* **18**: 25–33.

Lu M, Zhou X, Yang Q, Li H, Luo Y, Fang C, Chen J, Yang X, Li B. **2013**. Responses of ecosystem carbon cycle to experimental warming: a meta-analysis. *Ecology* **94**: 726–738.

Mäkelä A, Valentine HT, Helmisaari H-S. **2008**. Optimal co-allocation of carbon and nitrogen in a forest stand at steady state. *New Phytologist* **180**: 114–123.

McCree KJ. **1970**. An equation for the rate of respiration of white clover grown under controlled conditions. *Prediction and measurement of photosynthetic productivity. Proceedings of the IBP/PP Technical Meeting, Trebon, [Czechoslovakia], 14-21 September, 1969*.

McMurtrie RE, Dewar RC. **2013**. New insights into carbon allocation by trees from the hypothesis that annual wood production is maximized. *New Phytologist* **199**: 981–990.

Melillo JM, Butler S, Johnson J, Mohan J, Steudler P, Lux H, Burrows E, Bowles F, Smith R, Scott L, *et al.* 2011. Soil warming, carbon–nitrogen interactions, and forest carbon budgets. *Proceedings of the National Academy of Sciences* **108**: 9508–9512.

Melillo JM, Steudler PA, Aber JD, Newkirk K, Lux H, Bowles FP, Catricala C, Magill A, Ahrens T, Morrisseau S. **2002**. Soil Warming and Carbon-Cycle Feedbacks to the Climate System. *Science* **298**: 2173–2176.

Mencuccini M. **2003**. The ecological significance of long-distance water transport: short-term regulation, long-term acclimation and the hydraulic costs of stature across plant life forms. *Plant, Cell & Environment* **26**: 163–182.

Mensforth LJ, Thorburn PJ, Tyerman SD, Walker GR. **1994**. Sources of water used by riparian Eucalyptus camaldulensis overlying highly saline groundwater. *Oecologia* **100**: 21–28.

Mokany K, Raison RJ, Prokushkin AS. **2006**. Critical analysis of root : shoot ratios in terrestrial biomes. *Global Change Biology* **12**: 84–96.

Munir TM, Perkins M, Kaing E, Strack M. **2015**. Carbon dioxide flux and net primary production of a boreal treed bog: Responses to warming and water-table-lowering simulations of climate change. *Biogeosciences* **12**: 1091–1111.

Nemani RR, Keeling CD, Hashimoto H, Jolly WM, Piper SC, Tucker CJ, Myneni RB, Running SW. **2003**. Climate-Driven Increases in Global Terrestrial Net Primary Production from 1982 to 1999. *Science* **300**: 1560–1563.

Palmroth S, Oren R, McCarthy HR, Johnsen KH, Finzi AC, Butnor JR, Ryan MG, Schlesinger WH. **2006**. Aboveground sink strength in forests controls the allocation of carbon below ground and its [CO2]-induced enhancement. *Proceedings of the National Academy of Sciences* **103**: 19362–19367.

Pfautsch S, Dodson W, Madden S, Adams MA. **2015**. Assessing the impact of large-scale water table modifications on riparian trees: a case study from Australia. *Ecohydrology* **8**: 642–651.

Pfautsch S, Keitel C, Turnbull TL, Braimbridge MJ, Wright TE, Simpson RR, O'Brien JA, Adams MA. **2011**. Diurnal patterns of water use in Eucalyptus victrix indicate pronounced desiccation–rehydration cycles despite unlimited water supply. *Tree Physiology* **31**: 1041–1051.

van der Ploeg RR, Bo¨hm W, Kirkham MB. **1999**. On the Origin of the Theory of Mineral Nutrition of Plants and the Law of the Minimum. **63**: 1055–1062.

Poorter H, Jagodzinski AM, Ruiz-Peinado R, Kuyah S, Luo Y, Oleksyn J, Usoltsev VA, Buckley TN, Reich PB, Sack L. **2015**. How does biomass distribution change with size and differ among species? An analysis for 1200 plant species from five continents. *New Phytologist* **208**: 736–749.

Poorter H, Niklas KJ, Reich PB, Oleksyn J, Poot P, Mommer L. **2012**. Biomass allocation to leaves, stems and roots: meta-analyses of interspecific variation and environmental control. *New Phytologist* **193**: 30–50.

Poorter H, Sack L. **2012**. Pitfalls and Possibilities in the Analysis of Biomass Allocation Patterns in Plants. *Frontiers in Plant Science* **3**.

Pugh T a. M, Mueller C, Arneth A, Haverd V, Smith B. **2016**. Key knowledge and data gaps in modelling the influence of CO2 concentration on the terrestrial carbon sink. *Journal of Plant Physiology* **203**: 3–15.

Reich PB. **2002**. Root-shoot relations: Optimality in acclimation and adaptation or the 'Emperor's New Clothes. In: Plant roots: the hidden half. 205–220.

Reich PB, Luo Y, Bradford JB, Poorter H, Perry CH, Oleksyn J. **2014**. Temperature drives global patterns in forest biomass distribution in leaves, stems, and roots. *Proceedings of the National Academy of Sciences* **111**: 13721–13726.

Reich PB, Sendall KM, Stefanski A, Wei X, Rich RL, Montgomery RA. **2016**. Boreal and temperate trees show strong acclimation of respiration to warming. *Nature* **531**: 633–+.

Reichstein M, Falge E, Baldocchi D, Papale D, Aubinet M, Berbigier P, Bernhofer C, Buchmann N, Gilmanov T, Granier A, *et al.* 2005. On the separation of net ecosystem exchange into assimilation and ecosystem respiration: review and improved algorithm. *Global Change Biology* **11**: 1424–1439.

Roux XL, Lacointe A, Escobar-Gutiérrez A, Dizès SL. **2001**. Carbon-based models of individual tree growth: A critical appraisal. *Annals of Forest Science* **58**: 469–506.

Running SW, Gower ST. **1991**. FOREST-BGC, A general model of forest ecosystem processes for regional applications. II. Dynamic carbon allocation and nitrogen budgets. *Tree Physiology* **9**: 147–160.

Rustad L, Campbell J, Marion G, Norby R, Mitchell M, Hartley A, Cornelissen J, Gurevitch J, GCTE-NEWS. **2001**. A meta-analysis of the response of soil respiration, net nitrogen mineralization, and aboveground plant growth to experimental ecosystem warming. *Oecologia* **126**: 543–562.

Santiago LS, Wright SJ, Harms KE, Yavitt JB, Korine C, Garcia MN, Turner BL. **2012**. Tropical tree seedling growth responses to nitrogen, phosphorus and potassium addition. *Journal of Ecology* **100**: 309–316.

Sillmann J, Kharin VV, Zwiers FW, Zhang X, Bronaugh D. **2013**. Climate extremes indices in the CMIP5 multimodel ensemble: Part 2. Future climate projections. *Journal of Geophysical Research-Atmospheres* **118**: 2473–2493.

Sinclair TR, Horie T. **1989**. Leaf Nitrogen, Photosynthesis, and Crop Radiation Use Efficiency: A Review. *Crop Science* **29**: 90.

Smith NG, Dukes JS. **2013**. Plant respiration and photosynthesis in global-scale models: incorporating acclimation to temperature and CO2. *Global Change Biology* **19**: 45–63.

Strömgren M, Linder S. **2002**. Effects of nutrition and soil warming on stemwood production in a boreal Norway spruce stand. *Global Change Biology* **8**: 1194–1204.

Taeger S, Sparks TH, Menzel A. **2015**. Effects of temperature and drought manipulations on seedlings of Scots pine provenances. *Plant Biology* **17**: 361–372.

Thomas DS, Montagu KD, Conroy JP. **2007**. Temperature effects on wood anatomy, wood density, photosynthesis and biomass partitioning of Eucalyptus grandis seedlings. *Tree Physiology* **27**: 251–260.

Tjoelker MG, Oleksyn J, Reich PB. **1998**. Temperature and ontogeny mediate growth response to elevated CO2 in seedlings of five boreal tree species. *The New Phytologist* **140**: 197–210.

Tjoelker MG, Oleksyn J, Reich PB. **1999**. Acclimation of respiration to temperature and CO2 in seedlings of boreal tree species in relation to plant size and relative growth rate. *Global Change Biology* **5**: 679–691.

Volder A, Briske DD, Tjoelker MG. **2013**. Climate warming and precipitation redistribution modify tree–grass interactions and tree species establishment in a warm-temperate savanna. *Global Change Biology* **19**: 843–857.

Wang D, Maughan MW, Sun J, Feng X, Miguez F, Lee D, Dietze MC. **2012**. Impact of nitrogen allocation on growth and photosynthesis of Miscanthus (Miscanthus x giganteus). *Global Change Biology Bioenergy* **4**: 688–697.

Way DA, Oren R. **2010**. Differential responses to changes in growth temperature between trees from different functional groups and biomes: a review and synthesis of data. *Tree Physiology* **30**: 669–688.

Way DA, Yamori W. **2014**. Thermal acclimation of photosynthesis: on the importance of adjusting our definitions and accounting for thermal acclimation of respiration. *Photosynthesis Research* **119**: 89–100.

Zolfaghar S, Villalobos-Vega R, Zeppel M, Cleverly J, Rumman R, Hingee M, Boulain N, Li Z, Eamus D. **2017**. Transpiration of Eucalyptus woodlands across a natural gradient of depth-to-groundwater. *Tree Physiology* **37**: 961–975.